Distorted perovskite with e_g^1 configuration as a frustrated spin system

T. Kimura,[1,*] S. Ishihara,[2] H. Shintani,[1] T. Arima,[3] K. T. Takahashi,[1] K. Ishizaka,[1] and Y. Tokura[1]

[1]*Department of Applied Physics, University of Tokyo, Tokyo 113-8656, Japan*
[2]*Department of Physics, Tohoku University, Sendai 980-8578, Japan*
[3]*Institute of Materials Science, University of Tsukuba, Tsukuba 305-8573, Japan*

The evolution of spin- and orbital-ordered states has been investigated for a series of insulating perovskites $R\mathrm{MnO_3}$ ($R = \mathrm{La, Pr, Nd}, \ldots$). $R\mathrm{MnO_3}$ with a large $\mathrm{GdFeO_3}$-type distortion is regarded as a frustrated spin system having ferromagnetic nearest-neighbor and antiferromagnetic (AF) next-nearest-neighbor (NNN) interactions within a $\mathrm{MnO_2}$ plane. The staggered orbital order associated with the $\mathrm{GdFeO_3}$-type distortion induces the anisotropic NNN interaction, and yields unique *sinusoidal* and *up-up-down-down* AF ordered states in the distorted perovskites with e_g^1 configuration.

Common electronic characteristics exist in perovskite manganites $R\mathrm{MnO_3}$ and nickelates $R\mathrm{NiO_3}$ (R = trivalent lanthanoids). On the $\mathrm{Mn^{3+}}$ and $\mathrm{Ni^{3+}}$ sites with the $e_g^1 t_{2g}^3$ and $e_g^1 t_{2g}^6$ configurations, respectively, the e_g orbital is doubly degenerate and the t_{2g} orbital degree of freedom is quenched. It is widely recognized that the layered-type (A-type) antiferromagnetic (AF) structure in $\mathrm{LaMnO_3}$ is understood from the viewpoint of the anisotropic superexchange (SE) interaction under the directional order of orbital.[1,2] On the other hand, the spin structure in nickelates ($R \neq \mathrm{La}$) is distinct from the A-type AF; the so-called "up-up-down-down"-type one, where two Ni sites of "up" spins are followed by two sites of "down" spins along the principal axes in the cubic unit cell. Origin of this unusual magnetic order has been a long-standing question, as well as its relations to metal-insulator transition, orbital order (OO), and charge disproportionation.[3–5] Recently, a similar spin structure, i.e., the up-up-down-down order in a $\mathrm{MnO_2}$ plane (E-type AF order in the Wollan-Koehler notation[6]), is found in a manganite $\mathrm{HoMnO_3}$ (Ref. 7) with a significantly distorted perovskite structure. This has to be a bridge between the well-understood A-type AF in manganites and the unique magnetic ground state in nickelates.

In this Communication, we examine systematically the magnetic and orbital structures in a series of $R\mathrm{MnO_3}$ as a function of the ionic radius (r_R) of R. The most significant effect on the crystal structure by decreasing r_R is an enhancement of the cooperative rotation of the $\mathrm{MnO_6}$ octahedra (the $\mathrm{GdFeO_3}$-type distortion) characterized by the decrease of Mn-O-Mn bond angle ϕ. Let us first summarize in Fig. 1 the orbital (a) and spin (b) ordering temperatures (T_{OO} and T_{N}, respectively) on Mn sites of $R\mathrm{MnO_3}$ as a function of ϕ, which is based on both the present and the former studies.[7–10] Here, we adopt the ϕ at room temperature.[11] The T_{OO} monotonically increases with decreasing r_R, while the magnetic transition occurs from the A-type AF to the E-type one through the incommensurate structure. We argue that the combination of OO and next-nearest-neighbor (NNN) SE interaction brings about a nontrivial effect on the magnetic ground state in the systems with the orbital degeneracy and the large $\mathrm{GdFeO_3}$-type distortion. Microscopic calculation

shows that the magnetism in this system is mapped onto the frustrated spin model which well reproduces the phase diagram of $R\mathrm{MnO_3}$.

A series of $R\mathrm{MnO_3}$ ($R = \mathrm{La\text{-}Dy}$) crystals were grown by the floating zone method. We made powder x-ray-diffraction
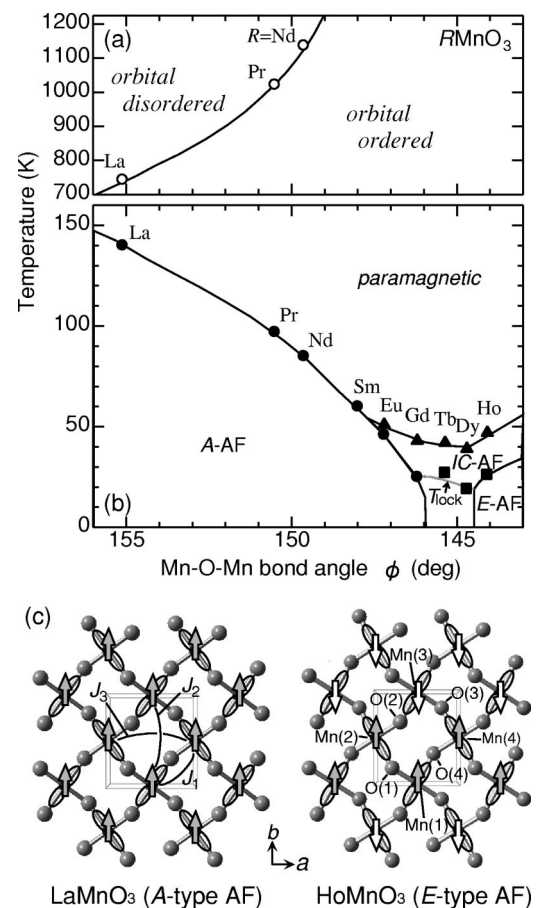

FIG. 1. Orbital (a) and spin (b) ordering temperatures of $R\mathrm{MnO_3}$ as a function of the in-plane Mn-O-Mn bond angle. (c) Crystal structures of $\mathrm{LaMnO_3}$ and $\mathrm{HoMnO_3}$. Spin (arrows) and orbital (lobes) ordered features are also illustrated. The stack of spin and orbital order along the c axis is staggered and uniform order, respectively, for both the compounds.
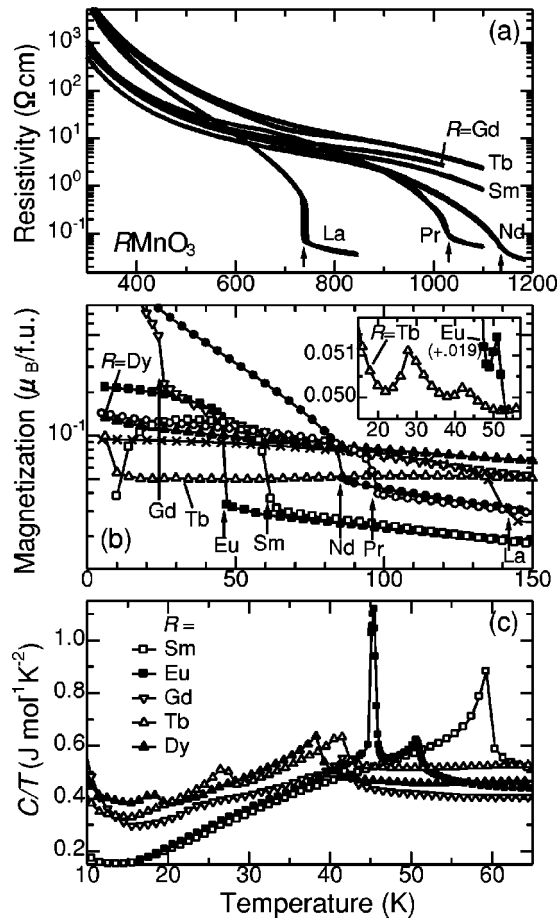
FIG. 2. Temperature profiles of (a) resistivity, (b) magnetization M, and (c) specific heat divided by temperature, C/T, for RMnO$_3$ crystals. Vertical arrows in (a) and (b) indicate T_{OO} and T_N for the Mn moment, respectively. The inset magnifies the M of R=Tb and Eu in the vicinity of T_N.

measurements on the obtained crystals at room temperature, and confirmed that all the crystals show the $Pbnm$ orthorhombic structure. Magnetization at 0.5 T was measured with a superconducting quantum interference device magnetometer. Specific heat was measured using a relaxation technique. Resistivity measurements were made by a standard four-probe method in a flow of Ar gas up to ~ 1200 K.

Let us show in Fig. 2 the experimental data [temperature (T) profiles of (a) resistivity ρ, (b) magnetization M, and (c) specific heat divided by temperature C/T], which compose the phase diagram of Figs. 1(a) and 1(b). As shown in Fig. 2(a), all the crystals show insulating behaviors over the whole T range investigated here. For a LaMnO$_3$ crystal, the ρ shows an abrupt drop toward high T at $T_{OO} \approx 747$ K in accordance with the cooperative Jahn-Teller (JT) or orbital-ordering transition.[12] With decreasing r_R, the anomaly in ρ, i.e., T_{OO}, is shifted toward higher T (indicated by arrows). In the crystals with smaller r_R than r_{Nd}, however, no such anomaly was observed up to 1500 K. Thus, the OO state associated with the cooperative JT distortion is extremely stable in RMnO$_3$ with small r_R.

As shown in Fig. 2(b), a steep rise of M toward lower T (indicated by vertical arrows) is observed in most of the crys-

tals. The anomaly in R=La-Nd crystals well corresponds to T_N for the A-type AF order.[6,8,9] The T_N falls monotonically with decreasing r_R from La to Gd. A similar jump of M attributed to the spin ordering of Mn site is not observed in R=Tb and Dy crystals with small r_R. (The anomaly in M below 10 K is related to the ordering of R-site f moment.) In TbMnO$_3$, however, the M exhibits two sharp peaks at ~ 42 K and ~ 27 K [the inset of Fig. 2(b)]. Figure 2(c) shows the C/T for crystals with smaller r_R. In SmMnO$_3$, the jump of C/T at ~ 59 K nicely agrees with the steep rise of M, and can be assigned to the A-type AF ordering. A remarkable feature in the C/T of EuMnO$_3$ is the sharp peak at ~ 46 K, as well as the jump at ~ 51 K. The sharp 46 K peak is suggestive of the first-order phase transition. In crystals with smaller r_R (R=Gd-Dy), a rather broader peak is observed at ~ 40 K. In addition, another broad peak feature is evident in the T region 18–26 K. Among them, the T evolution of spin structure has been investigated for TbMnO$_3$ by neutron-diffraction measurements.[10] The observed peaks in C/T and M at ~ 42 K for TbMnO$_3$ correspond to the onset of the sine-wave ordering of the Mn moments with the wave vector of $(0,k_s,0)$. The $k_s (\sim 0.295)$ at T_N is incommensurate (IC) and decreases with decreasing T, and becomes nearly constant ($k_s = 0.28$) below ~ 30 K. The anomalies in C/T and M at ~ 27 K are in good agreement with the T where k_s is locked at a constant value (T_{lock}). With further decreasing r_R, Muñoz *et al.*[7] reported that in polycrystalline HoMnO$_3$ ($T_N = 41$ K), the IC-to-commensurate (CM) magnetic phase transition takes place at ~ 26 K, where the wave vector is $(0,k_s,0)$ [$0.4 \leqslant k_s < 0.5$ (T dependent) for the IC phase and $k_s = \frac{1}{2}$ for the CM one].

As displayed in Fig. 1, T_{OO} steeply increases with decreasing ϕ, whereas T_N for the A-type AF order monotonically decreases. With the suppression of the A-type AF order, the IC sinusoidal magnetic structure which propagates along the b axis appears. With further decreasing ϕ, the CM magnetic structure with the wave vector of $(0,\frac{1}{2},0)$ turns up at the ground state in HoMnO$_3$.[7] The CM magnetic structure can be identified with the "up-up-down-down" spin structure within the ab plane or the E-type AF structure. To visualize the modification of the crystallographic and magnetic structures by the decrease of ϕ, we illustrate in Fig. 1(c) the projection of the fundamental crystal structure of LaMnO$_3$ and HoMnO$_3$ along the c axis.

In RMnO$_3$ with a small GdFeO$_3$-type distortion, such as LaMnO$_3$, the staggered $[d_{3x^2-r^2}/d_{3y^2-r^2}]$-type OO is responsible for the A-type AF order. There are the ferromagnetic (FM) SE interaction between nearest-neighbor (NN) e_g spins and the AF one ($J_{AF}^{t_{2g}}$) between NN t_{2g} spins. The latter is superior along the c axis.[2] In RMnO$_3$ with significant GdFeO$_3$-type distortion (small r_R), the FM SE interaction is weakened due to reduction of the transfer intensity of an e_g electron. However, such an argument based on the NN interactions is not enough to explain the E-type AF or sinusoidal magnetic order; the inversion symmetry of the spin alignment is broken in the ab plane for the E-type AF structure, in
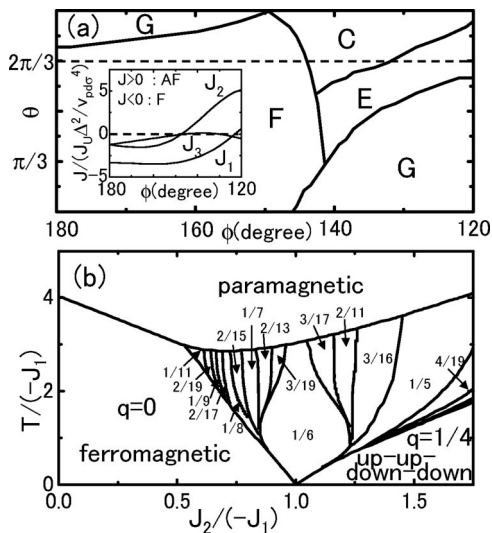
FIG. 3. (a) Magnetic phase diagram at $T=0$. θ is the orbital-mixing angle. The broken line indicates the $[d_{3x^2-r^2}/d_{3y^2-r^2}]$-type orbital order. C, E, G, and F imply the C-, E-, G-type antiferromagnetic (AF) and FM phases, respectively (Ref. 16). The inset shows the effective superexchange interactions between nearest-neighbor Mn spins (J_1), next-nearest-neighbor (NNN) Mn spins along the b axis (J_2), and NNN Mn spins along the a axis (J_3) at $\theta=2\pi/3$ (Ref. 15). (b) Mean-field magnetic phase diagram of the 2D J_1 $-J_2-J_3$ model with $J_3/J_1=0.01$. Each phase is characterized by a wave number $q=M/N$ of the spin structure along the b axis. $q=0$ and 1/4 correspond to the A- and E-type AF states in RMnO$_3$, respectively.

spite of the fact that the two NN bonds along the opposite directions are equivalent from the crystal structural point of view.

The crucial effect caused by the significant GdFeO$_3$-type distortion is the SE interaction between NNN Mn sites. It is evident in Fig. 1(c) that the enhancement of the GdFeO$_3$-type distortion shortens the distance between O(2) and O(4) [e.g., the O(2)-O(4) length is ≈ 3.4 Å for LaMnO$_3$ and ≈ 3.0 Å for HoMnO$_3$ at room temperature[11]]. This shortening enhances the SE interaction between NNN sites through Mn-O(2)-O(4)-Mn exchange paths. Under the staggered OO, in addition to the GdFeO$_3$-type distortion, the two NNN SE interactions along the different directions become inequivalent; the interaction between Mn(1) and Mn(3) (along the b axis) is stronger than that between Mn(2) and Mn(4) (along the a axis). Since the occupied orbitals in Mn(1) and Mn(3) are the same, this SE interaction is the AF one which brings about the spin frustration.

We present the theoretical prescription for the combination effect of the GdFeO$_3$-type distortion and the staggered OO. The Hamiltonian adopted here is the spin-orbital model which is known to describe well the orbitally degenerate manganites,[2] $\mathcal{H}=\mathcal{H}_J+\mathcal{H}_H+\mathcal{H}_{AF}$. The main term $\mathcal{H}_J$ is the exchange interaction between intersite e_g spins and orbitals schematically written as $\mathcal{H}_J=\Sigma_m J_m \Sigma_{\langle ij \rangle}(a_m\vec{S}_i\cdot\vec{S}_j +b_m)h_m(\vec{T}_i,\vec{T}_j)$. m is an index classifying the exchange processes, J_m indicates the SE interactions, a_m and b_m are the constants, and $\vec{S}_i$ is the spin operator of the e_g electron.
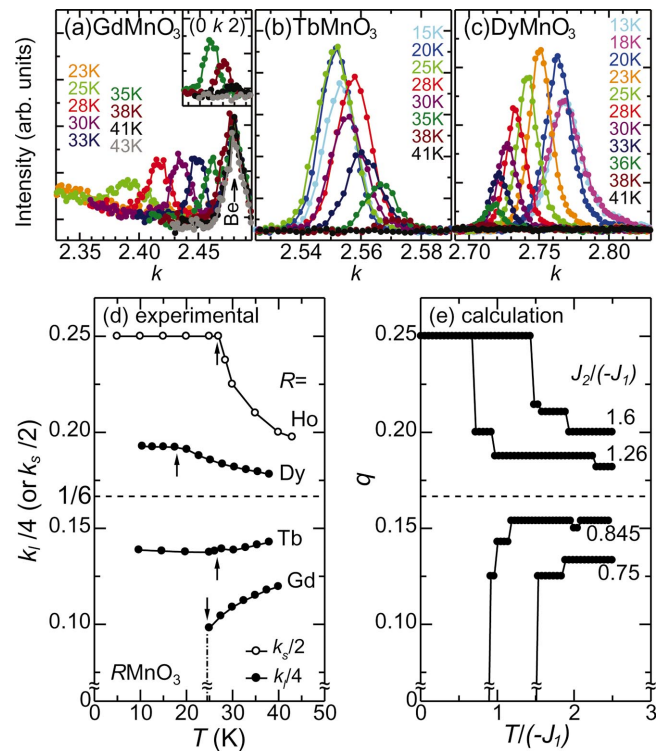

FIG. 4. (Color) (a)–(c): X-ray-diffraction k scans along (0,k,3) at various T for $R=$Gd, Tb, and Dy crystals, measured at BL-4C of PF-KEK, Tsukuba. T profiles of the wave number of modulated magnetic structure obtained by (d) experiment and (e) calculation. The arrows denote T_{lock}. The data of k_s in HoMnO$_3$ were taken from Ref. 7.

The orbital part $h_m(\vec{T}_i,\vec{T}_j)$ is represented by the pseudospin operator $\vec{T}_i$ with a magnitude 1/2. $\mathcal{H}_H$ and $\mathcal{H}_{AF}$ in $\mathcal{H}$ are the Hund coupling between e_g and t_{2g} spins, and the AF interaction $J_{AF}^{t_{2g}}$ between NN t_{2g} spins, respectively. Beyond the conventional spin-orbital model, the SE interactions between NNN Mn sites are considered in $\mathcal{H}_J$. The effective electron transfer $t_{ij}^{\gamma\gamma'}$ between i and j Mn sites with γ and $\gamma'(=3z^2-r^2,x^2-y^2)$ orbitals occurs through the O $2p$ orbitals.[13] For example, for the Mn(1)-Mn(3) pair [see Fig. 1(c)], possible exchange paths are [Mn(1)$-$O(1),O(4)$-$O(2),O(3) $-$Mn(3)]. Both the GdFeO$_3$-type and JT-type distortions are introduced in $t_{ij}^{\gamma\gamma'}$ through the Slater-Koster formulas.[14]

The magnetic phase diagram is calculated by the mean-field approximation at $T=0$ [Fig. 3(a)] (Refs. 15,16) in the two-dimensional (2D) square lattice, since the AF spin alignment along the c axis due to $J_{AF}^{t_{2g}}$ remains unchanged in a series of RMnO$_3$. The staggered OO with two sublattices is of the $[\theta/-\theta]$-type characterized by the mixing angle: $|\theta\rangle=\cos(\theta/2)|d_{3z^2-r^2}\rangle+\sin(\theta/2)|d_{x^2-y^2}\rangle$. The $[d_{3x^2-r^2}/d_{3y^2-r^2}]$-type OO corresponds to $\theta=2\pi/3$. Without the GdFeO$_3$-type distortion, the FM order in the ab plane, corresponding to the A-type AF order in the three-dimensional lattice, appears for $\theta<1.75\pi$. With decreasing ϕ, the E-type AF phase of the present interest appears for $1.75\pi<\theta<2.5\pi$ and $\phi<143°$. This result agrees semiquantitatively with the experiments. The remarkable change with

decreasing ϕ is seen in the SE interaction between Mn(1) and Mn(3) along the b axis; it turns to a strong AF interaction from a weak FM one [see J_2 in the inset of Fig. 3(a)] as well as weakening of the NN FM one (J_1).[17,18]

The essence of magnetic properties in this system is mapped onto the 2D frustrated Heisenberg model for $S=2$ with FM NN interaction (J_1), AF NNN one along the b axis (J_2), and weak FM NNN along the a axis (J_3). The finite T phase diagram is obtained by the mean-field approximation [Fig. 3(b)]. A periodicity N of the spin structure is taken up to 20 along the a, b, and $a\pm b$ directions, and each phase is characterized by the wave number $q=M/N$. The phase diagram shows a similar topological structure to that in the axial next-nearest-neighbor Ising model;[19,20] numerous long-range orders between the FM ($q=0$) and up-up–down-down-type AF ($q=1/4$) phases, which is the so-called Devil's flower. The calculated results qualitatively reproduce the phase diagram of RMnO$_3$ in Fig. 1(b). (Note that the A-type AF state is regarded as the 2D FM state.)

Further supporting evidence is needed to confirm the validity of the present scenario. However, it is difficult to investigate the spin structure by the neutron diffraction for compounds with Gd and Dy elements because of their large neutron-scattering cross sections. Hence, we overcome the problem by measurements of single-crystal x-ray diffraction. Figures 4(a)–4(c) show x-ray-diffraction scans along (0,k,3) at various T for $R=$ Gd, Tb, and Dy crystals.[21] For all the crystals, additional superlattice peaks appear at the wave vector (0,k_l,l) for integer l below T_N. In TbMnO$_3$, the k_l is ~ 0.57 at $T_N\sim 40$ K, decreases with decreasing T, and becomes nearly constant ($k_l\sim 0.55$) below $T_{lock}\sim 27$ K. The

value of T-dependent k_l is almost twice as large as that of k_s. It is well known that the crystallographic deformations at magnetic ordering are due to the *exchange striction*.[22] The observed superlattice reflections due to the atomic displacement can be regarded as the second harmonic peaks magnetoelastically induced by sinusoidal AF order. Hence, a half value of k_l could represent k_s. The T profiles of the wave number $k_s=k_l/2$ obtained by experiments are compared with those calculated for the representative values of $J_2/(-J_1)$ [Figs. 4 (d) and 4(e)]. The theoretical results are in quantitatively good agreement with experiments in terms of T and R dependence, which strongly suggests that the present modeling approach is proper for understanding the phase diagram of RMnO$_3$.

We examined the evolution of magnetic and orbital states in a series of RMnO$_3$ as a function of the ionic radii r_R in R. The T_N of the A-type AF order steeply decreases with the decrease of r_R. Eventually the up-up-down-down type (E-type) AF order appears in $R=$ Ho via the sinusoidal magnetic order in $R=$ Tb. Such curious AF ordered states in RMnO$_3$ can be explained in a scenario of the spin frustration caused by the combination of the significant GdFeO$_3$ distortion and the staggered OO; the former enhances the NNN SE interaction, and the latter causes the anisotropy in the NNN SE interaction. This scenario can also be applicable to the up-up-down-down AF order observed in RNiO$_3$ with the distorted perovskite structure.

*Present address: Los Alamos National Laboratory, Los Alamos, NM 87545.

[1] K.I. Kugel and D.I. Khomskii, Zh. Eksp. Teor. Fiz. **64**, 1429 (1973) [Sov. Phys. JETP **37**, 725 (1973)]; Usp. Fiz. Nauk **136**, 621 (1982) [Sov. Phys. Usp. **25**, 231 (1982)].

[2] S. Ishihara *et al.*, Phys. Rev. B **55**, 8280 (1997).

[3] J.L. García-Muñoz *et al.*, Phys. Rev. B **50**, 978 (1994).

[4] J.A. Alonso *et al.*, Phys. Rev. Lett. **82**, 3871 (1999).

[5] T. Mizokawa *et al.*, Phys. Rev. B **61**, 11 263 (2000).

[6] E.O. Wollan and W.C. Koehler, Phys. Rev. **100**, 545 (1955).

[7] A. Muñoz *et al.*, Inorg. Chem. **40**, 1020 (2001).

[8] Z. Jirak *et al.*, J. Magn. Magn. Mater. **53**, 153 (1985).

[9] S.Y. Wu *et al.*, J. Appl. Phys. **87**, 5822 (2000).

[10] S. Quezel *et al.*, Physica B **86-88**, 916 (1977).

[11] J.A. Alonso *et al.*, Inorg. Chem. **39**, 917 (2000). (We use ϕ of $R=$ Sm, Eu, and Gd samples by interpolating from a nearly linear relation between ϕ and r_R.)

[12] J. Rodríguez-Carvajal *et al.*, Phys. Rev. B **57**, R3189 (1998).

[13] $t_{ij}^{\gamma\gamma'}$ between NN and NNN sites are given by $(1/\Delta)\Sigma_{k\alpha}t_{ki}^{p_\alpha d\gamma}t_{kj}^{p_\alpha d\gamma'}$ and $(1/\Delta^2)\Sigma_{kl\alpha\beta}t_{ki}^{p_\alpha d\gamma}t_{kl}^{p_\alpha p_\beta}t_{lj}^{p_\beta d\gamma'}$, respectively, with the charge transfer energy Δ, and the transfer inte-

gral between Mn $3d$(O$2p$) and O$2p$ ions $t_{ki}^{p_\alpha d\gamma}(t_{kl}^{p_\alpha p_{\alpha'}})$.

[14] J.C. Slater and G.F. Koster, Phys. Rev. **94**, 1498 (1954).

[15] We chose the charge transfer energy $\Delta=2$ eV, the transfer integral between $3d$ and $2p$ orbitals $v_{pd\sigma}=-1.58$ eV, that between $2p$ orbitals $v_{pp\sigma}=0.5$ eV, $J_{U'-I}/J_U=3$, and $J_{AF}^{t_{2g}}/J_U=0.01$, where $J_{U'-I}$ and J_U are the SE interactions in $\mathcal{H}_J$.[2]

[16] Six spin structures are assumed in the 2D lattice: the FM structure (F), the checker board-type AF one (G), the chain-type AF ones along the a-b axis (C) and that along the $a+b$ axis (C'), and the up-up-down-down-type AF ones with the zigzag chains along the a axis (E) and that along the b axis (E').

[17] L.E. Gontchar and A.E. Nikiforov, Phys. Rev. B **66**, 014437 (2002).

[18] T. Hotta *et al.*, Phys. Rev. Lett. **90**, 247203 (2003).

[19] P. Bak and J. von Boehm, Phys. Rev. B **21**, 5297 (1980).

[20] P. Bak, Rep. Prog. Phys. **45**, 587 (1982).

[21] Since the diffraction by a Be window overlaps that of the superlattice at (0,k,3) near T_N for GdMnO$_3$, we show in the inset of Fig. 4(a) (0,k,2) scans near T_N.

[22] J.S. Smart and S. Greenwald, Phys. Rev. **82**, 113 (1951).